Electric Power Systems Research 206 (2022) 107783

Contents lists available at ScienceDirect

Electric Power Systems Research

journal homepage: www.elsevier.com/locate/epsr

Assessment and Enhancement of Hopf Bifurcation Stability Margin in Uncertain Power Systems

Ram Krishan [*,a], Ashu Verma [b]

[a] National Institute of Technology Warangal, India
[b] Indian Institute of Technology Delhi, India

ARTICLE INFO

Keywords:
Boundary Eigenvalue
Hopf Bifurcation
Optimization
Small-signal stability
Stability Margin
Non-Statistical Uncertainties

ABSTRACT

Uncertainties in the forecasted load and generation can have a catastrophic impact on power system stability. For a reliable power supply, a sufficient dynamic stability margin is always desired. This paper introduces a novel boundary eigenvalue-based approach for the determination of Hopf Bifurcation Stability Margin (HBSM), which, explicitly, accounts for the impact of uncertainties in specified renewable generation and loads. Since the Hopf bifurcation stability problem is nondeterministic, it requires large computational efforts to determine the HBSM. Most of the available methods are based on statistical data, which are computationally less efficient for such applications. In this paper, a non-statistical uncertainty based control rescheduling strategy is proposed to enhance the stability margin of the system. To balance the trade-off between solution quality and computation time, the proposed approach is composed of two stages: i) determination of boundaries of critical eigenvalues; and ii) optimal setting of the controllers by minimization of a boundary active power loss based objective function under the given range of uncertainties. The proposed approach is demonstrated on standard IEEE test systems with promising results to show the importance and its reliability.

1. Introduction

1.1. Motivation

The oscillatory stability problem is an inherent non-linear phenomenon that relates to Hopf Bifurcation (HB) of dynamic power systems. Modern power systems are forced to operate with substantially small stability margins due to financial, environmental, and other constraints. Such a power system can be driven to one of the most prominent oscillatory instability problems due to successively increase or decrease in loads, especially, when systems are integrated with intermittent Renewable Energy Sources (RES). HB instability is detected before the Saddle Node Bifurcation (SNB) point. Therefore, assessment and enhancement of HBSM are essential for a reliable and secure power system operation. HB instability is caused by several reasons, including variation in operating conditions, load/ generation information, and setting of power system controllers. Therefore, it is necessary to ensure the sufficient HBSM in the large and uncertain power system [1].

1.2. Literature review

In the last few decades, various methods have been proposed to enhance the oscillatory stability margin of the interconnected power system. An online line switching method has been proposed for the enhancement of small-signal stability margin. Though the switching method has a good trade-off between speed and solution quality, it had not accounted for the uncertainties in input data [2]. Recently, Rekasius substitution-based an efficient method has been proposed for computing the delay margins of power system [3]. Taking advantage of the quantitative relationship between stability margin and the control variables, an online preventive control method for static voltage stability is proposed in [4]. The computation time of this method is quite good for finding the trajectory of eigenvalues with deterministic data. In [5]-[6], the authors propose to use power system controllers for the enhancement of oscillatory stability. Moreover, a coordinated robust control method has been proposed in[7] to enhance the dynamic stability of RES integrated power system. In [8], a machine learning-based approach has been proposed for quantifying the stability margin of power systems reflecting dynamics of wind power generation. These controllers are mostly designed offline with consideration of one or few operating

* Corresponding author.
E-mail address: rkrishan@nitw.ac.in (R. Krishan).

https://doi.org/10.1016/j.epsr.2022.107783
Received 15 May 2021; Received in revised form 6 September 2021; Accepted 6 January 2022
Available online 15 January 2022
0378-7796/© 2022 Elsevier B.V. All rights reserved.

points, which may fail to damp out the system oscillations for other operating conditions reached under uncertainties. HB point of the system under forecasted load/generation data is the best indicator to identify the worst-case scenario of the system which can occur and should be used for enhancement of Small-Signal Stability Margin (SSSM).

In the last years, the tasks of monitoring and enhancing the stability margin related to SNB and HB have been done in proposed methods that deal with uncertainties in the direction of load growth. In [9–11], the authors proposed various methodologies to evaluate the loading margin related to voltage instability (SNB). To improve the HB limits/SSSM, and hence loadability of dynamic power systems, rescheduling of control parameters is one of the most effective ways[2]. In [12], controller rescheduling and generation re-dispatch have been used for minimization of power losses and enhancement of the system loading capability, where uncertainties are ignored. However, uncertainty must be considered in any power system analysis and control. In the literature, two different approaches, statistical and non-statistical, have been reported to deal with uncertainties in the forecasted/estimated data. In some of the recent researches presented in [13–15] have been assessed the small-signal stability of the uncertain power system, where, the slowest form of stability and the snapshot scenario of the system is considered in a direction of load increase.In[16], authors have been developed a promising stability margin monitoring system related to both SNB and HB based on load growth directions of the power system. However, deterministic models are used which requires a continuous stability margin assessment to capture the uncertainties in the estimated load growth direction. Statistical uncertainties in the load/generation data have been considered in these papers which requires a cumbersome computation [17] in the evaluation of stability margin. Therefore, these methods are less efficient for online implementation. Whereas non-statistical uncertainties-based approaches are computationally more efficient [18], [19], and can be used for online applications. Eigenvalue analysis being an important tool for assessing and improving the HB stability, it should be modified to consider these uncertainties to ensure the stable operation of power systems [1].

In [20],[21], probabilistic methods have been used for HBSM of an uncertain power system, whereas the Monte Carlo Method has been used in [22]. Analytical methods, such as cumulant-based methods and collocation methods have been presented in [23],[24] which are more efficient than the probabilistic methods. However, these traditional methods of Small Signal Stability Analysis (SSSA) are based on deterministic (crisp) load/generation data. The power system operator/designer is never sure of the exact load/generation scenario for the analysis. However, it is comparatively easy to give a reasonably accurate range of data for the analysis, operation, and control. This range of uncertainties has been used for different applications of the power system in [25],[26]. For the secure operation of the power system under the forecasted load/generation data, evaluation of dynamic loadability/HB stability limit is very important, as modern power systems are generally operated with very little stability margin. This problem can be mitigated by knowing the effective HB margin and rescheduling the available controls. Hence, the need to develop an effective control technique to avoid the instability caused by a small disturbance in the presence of various uncertainties is realized. The method to identify worst-case scenarios which can occur under a given range of uncertainty and their impact on HB point are given in [1]. Here, a sensitivity-based boundary eigenvalue approach is used to analyze the worst instability cases in advance.

1.3. Contribution and paper organization

In fact, related works over the last two-three decades reveal the effectiveness of re-dispatching of voltages and transformer taps in providing the promising solution for various power system challenges like reducing transmission loss, generation cost, assisting voltage stability and relieving line overloading etc. [27–30]. Most of the methods available in the literature are based on crisp data. These controllers are very less discussed in the past research for HBSM/HB limits enhancement especially with non-deterministic parameters. This paper seeks to fill the gap by considering the possible range of uncertainties in estimated power system parameters. In this paper, the authors propose an approach for the assessment and enhancement of HBSM via rescheduling of control settings in uncertain power systems. The major contributions of this paper are:

1. A rigorous formulation of the look-ahead assessment of worst-case scenarios for estimated/predicted/ forecasted loads using boundary eigenvalue approach.
2. A promising formulation of HBSM enhancement problem as an optimization problem using boundary active power loss evaluation and look-ahead approach, where, optimal rescheduling of power system controllers is carried out under non-statistical load/generation uncertainties of the interconnected power system.
3. The proposed approach has been applied and evaluated with different standard IEEE test systems.

This formulated optimization problem is solved by Gray Wolf Optimization (GWO) algorithm because it is less dependent on algorithmic parameters. Also, due to the leader selection-based mechanism, this algorithm has good convergence [31]. However, any other suitable optimization algorithm can also be used.

The organization of the remaining paper is as follows: In Section 2, theoretical background of the proposed approach, critical mode, and HBSM are discussed. The non-statistical uncertainty modelling of the electrical power system is discussed in Section 3. Boundary eigenvalue analysis and consideration of system uncertainties are also described in this section. Section 4 describes the problem formulation, boundary active power loss (BAPL) calculation, and optimization algorithm. Results and discussions for standard test systems are given in Section 5. Conclusions and future works are drawn in the Section 6.

2. Background of the proposed formulation

Hopf Bifurcation instability is mainly concerned with gradual variation either in operating parameters or in system parameters. These parameters are known as HB parameters. This paper aims at the HB stability analysis of large power systems subject to forecasted uncertainties in load/generation. In the proposed approach, concerns related to secure operation and design of the real-time power system having critical HBSM are addressed through the optimal control action to postpone the oscillatory instability due to change in parameters under an uncertain environment.

For a given change in control parameters i.e. generator re-dispatch, generator excitation (voltage control), and tap settings of tap changing transformers, there is a considerable impact on Hopf Bifurcation stability and Saddle Node Bifurcation (related to voltage instability). Rescheduling of the control parameters provides the stability margin change for any perturbation in the HB parameters. The solution to the rescheduling problem is always on the bifurcation boundaries. However, load-generation in modern power systems is not known with the complete certainties, there is always a chance of error in input parameters.

With the increase in load demand, power losses are increased and system operating points change accordingly. This change in operating point can affect the oscillatory stability margin (HB limit). The minimization of loss to enhance the HB limits gives more or less the same results obtained by minimization of the rightmost electromechanical eigenvalue-based objective function with simple calculations.Modern power systems are forced to operate near the critical loading with a very small stability margin. In such a stressed operating scenario, monitoring of HB limits and their enhancement become a big challenge for the system operator. In this critical zone, power system behaviour is highly non-linear, and the HB limit enhancement problem becomes quite

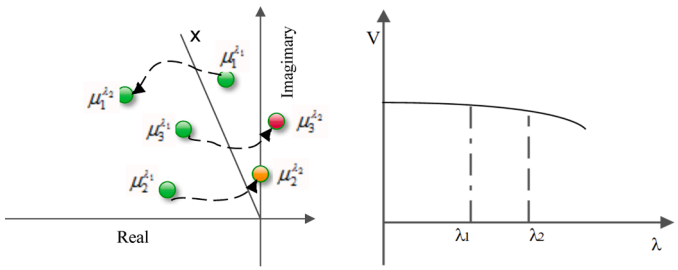

(a) S-domain (b) Load level domain

Fig. 1. Movement of eigenvalues (μ) and voltage drop with consecutive load steps λ_1 and λ_2

difficult. Reactive power limits are known to cause SNB stability problems in the power system. Generally, reactive power optimization problems are solved for the local requirement [12]. Moreover, the setting of power system control variables, generator voltages, and taps can be rescheduled optimally within their limits for enhancement of the HB limit. Hence, the effective utilization of available controls may allow accommodating the next predicted load without any cost augmentation. The philosophy of the look-ahead concept is used in this paper to enhance the HBSM via control rescheduling. To achieve a realistic solution, forecast uncertainties in load and solar photovoltaic generation are accounted for using the boundary eigenvalue approach. In this paper, only reactive controls are rescheduled. However, when it is ascertained that the system cannot serve predicted load due to imminent oscillatory instability, generation rescheduling can be used to enhance the HB limit and check the possibility to accommodate the next predicted load demands. It is important to mention that, as generation rescheduling influences the cost of operation, it is generally preferred when reactive controls are insufficient. Further, when rescheduling of active and reactive power is insufficient, load shedding can also be initiated to prevent instability. The real power control and load shedding scenarios have not been discussed in this paper.

2.1. Critical mode and HB Stability margin

Oscillatory stability of the dynamic power system can be analyzed by eigenvalues (μ) of the system matrix 'A_{sys}' at a specified operating state. In S-domain, critical eigenvalues (μ) are evaluated to numerically identify the stability margin of the system. The critical electromechanical mode (rightmost eigenvalue), say $\mu_{critical}$, is important to study the stability behaviour and HB margin[32]-[33]. In heavily stressed power systems, Hopf bifurcations occur when the eigenvalue of the system matrix cross over the imaginary axis (right half plan) due to a small deviation in the HB parameter(s). An illustration of eigenvalue movement with respect to change in HB parameter 'λ' is shown in Fig. 1a. At HB point (λ_{HB}), the system may lead to undamped oscillations. Load versus voltage profile of the system is also depicted in Fig. 1b to show the effect of loading on system operating points.

HB stability margin (λ_{HBSM})in terms of the loading capacity of the system can be measured by

$$\lambda_{HBSM} = \lambda_{HB} - \lambda;\ \forall \sigma_{crit} \leq 0 \tag{1}$$

Where λ_{HB} is the critical loading at the given operating point and σ_{crit} is the real part of the critical mode ($\mu_{critical}$). If the real part of critical eigenvalue is greater than zero (i.e. $\sigma_{crit} > 0$), the system is unstable with zero or negative stability margin. To ensure the dynamic stability of the stressed power system, it is important to keep the sufficient HBSM in all operating scenarios including the case of system uncertainties.

3. Mathematical modeling of power system

3.1. Power system DAE model

For oscillatory stability analysis, power system can be mathematically modelled by a set of nonlinear differential algebraic equations (DAE) including load flow equations. A non-statistical uncertainty based DAE model for HB stability analysis can be given as

$$\begin{aligned} \dot{\mathbf{X}} &= f(X, Y, \lambda, \mathscr{L}) \\ 0 &= g(X, Y, \lambda, \mathscr{L}) \end{aligned} \tag{2}$$

Where,f and g are the set of non-linear differential and network algebraic equations respectively.The $X \in R^n$and $Y \in R^m$ are the vector of state and algebraic variable respectively; $\lambda \geq 0$ is the parameter to represent the load/generation level in the system. It is also known as the hopf bifurcation parameter. The range of uncertainty is denoted by $\mathscr{L}$ in percentage. Here, $\mathscr{L} = 0\%$ (no uncertainty) indicates the crisp load/generation data. The effect of on-load tap changer and generator excitation control is accounted in (2) by rescheduling the taps and excitation control points during equilibrium testing using a look-ahead approach. Although other dynamic devices such as active power control, HVDCs, flexible ac transmission system (FACTS) are not explicitly considered here, they could be easily included in (2).

3.2. State Space Model

State-space model is obtained by linearization of (2) for power system SSSA at specified operating point (λ) and it can be given as [5].

$$A(\lambda, \mathscr{L}) = \begin{bmatrix} f_x(\lambda, \mathscr{L}) & f_y(\lambda, \mathscr{L}) \\ g_x(\lambda, \mathscr{L}) & g_y(\lambda, \mathscr{L}) \end{bmatrix} \tag{3}$$

Where augmented matrix $A(\lambda, \mathscr{L})$ is a sparse matrix which, elements are varied with operating point λ and specified level of uncertainty $\mathscr{L}$. Further, if g_y is a nonsingular matrix, reduced system matrix A_{sys} can be derived as

$$A_{sys}(\lambda, \mathscr{L}) = f_x(\lambda, \mathscr{L}) - f_y(\lambda, \mathscr{L}) g_y^{-1}(\lambda, \mathscr{L}) g_x(\lambda, \mathscr{L}) \tag{4}$$

Eigenvalues of A_{sys} determine the dynamic stability and HB limits of the system. For large power system, (4) is widely accepted [34] for eigenvalue analysis.

3.3. Boundary eigenvalue [1]

Worst case scenario of the uncertain power system can be investigated with the results of boundary eigenvalue analysis (BEA). A brief description of BEA is given in this section; however, a detailed description can be found in [1]. Using the power system model derived in section 3, λ_{HB} is evaluated by increasing loading factor λ in small steps till critical eigenvalue (lower boundary) crosses the imaginary axis. At each loading step and specified control settings, the lower boundary of the critical eigenvalue is calculated. At normal small signal stability, the real part of right most eigenvalue (σ_{crit}) must lies in the left half of the s-plane i.e $\sigma_{crit} < 0$ for all $\lambda < \lambda_{HB}$. At λ_{HB}, σ_{crit} is very close to the imaginary axis ($\sigma_{crit} = 0$). If the control setting is altered so that $\sigma_{crit} < 0$, then the HBSM of the system will be increased. For the obtained control settings, sensitivity of critical eigenvalue with respect to uncertain parameters P_L is evaluated by

$$C = \frac{\partial \sigma_{crit}}{\partial P_L} \tag{5}$$

Where C is the matrix of critical eigenvalue sensitivity. The limit (lower/upper) at which a variable of concern denoted by σ_{crit} is constrained, dictates whether the lower/upper boundary value is of interest. For desired boundary value of σ_{crit} under the specified range of

uncertainty, input vector $P_{select,j}{}'$ is selected according to the sign of the associated sensitivity element, C_j, that can be given as

If upper value of σ_{crit} is desired then

$$\sigma_{(crit,upper)} = \begin{cases} \sigma^0_{crit} + \sum_{j=1}^{n} C_j \left(P^{max}_{select,j} - P^0_{Lj} \right) & ;\ if\ C_j\ is\ negative \\ \sigma^0_{crit} + \sum_{j=1}^{n} C_j \left(P^{min}_{select,j} - P^0_{Lj} \right) & ;\ if\ C_j\ is\ positive \end{cases} \tag{6}$$

Similarly, for desired lower value of σ_{crit}

$$\sigma_{(crit,lower)} = \begin{cases} \sigma^0_{crit} + \sum_{j=1}^{n} C_j \left(P^{max}_{select,j} - P^0_{Lj} \right) & ;\ if\ C_j\ is\ positive \\ \sigma^0_{crit} + \sum_{j=1}^{n} C_j \left(P^{min}_{select,j} - P^0_{Lj} \right) & ;\ if\ C_j\ is\ negative \end{cases} \tag{7}$$

Where, σ^0_{crit} is the critical eigenvalue calculated at P^0_L and P^0_L is the vector of load specifications at the base case. $P^{max}_{select,j}$ and $P^{min}_{select,j}$ are the elements of selected vector $P_{select,j}{}'$ from the specified range of input variable (i.e. $[P_{Lmin}, P_{Lmax}]$). In the proposed approach, the lower boundary of σ_{crit} would be of interest and it must satisfy the inequality constraints in (13). Therefore, (7) has an important role in the calculations of λ_{HB}.

3.4. Uncertainties Consideration

In the power system, loads are neither controlled nor can be forecasted with complete certainty. However, it is much easier to specify the forecasted data in a certain range rather than the deterministic value. Here, uncertain loads are specified in the reasonable range $[P_{Lmin}, P_{Lmax}]$ by considering a few percent of forecast uncertainty in the given load data.

In this paper, uncertainty in distributed solar photovoltaic generations (SPVGs) is also considered. We assume that concentrated SPVGs are integrated at a few buses in the network where lumped loads are connected. Tamimi and Bhattacharya have advocated in [35] that distributed SPVG less efficient to voltage control at the point of common coupling. Therefore, this SPVG output can be taken as a negative load to account for the effect of SPVG in the operation. If the specified range of uncertainty in SPVG output is given as

$$P^{min}_{SPVG} \le P_{SPVG} \le P^{max}_{SPVG} \tag{8}$$

Then the uncertainty range at the SPVG connected bus is modified as

$$\begin{cases} P^{'}_{Lmin} = P_{Lmin} - P^{max}_{SPVG} \\ P^{'}_{Lmax} = P_{Lmax} - P^{min}_{SPVG} \end{cases} \tag{9}$$

Therefore, the effective uncertainty range may differ at load bus having SPVG.

3.5. Load Parameters and Generator participation

In the realistic power system, some of the generator units have capability to continuously modify their active power generation and participated in the generation re-dispatch. Such units are referred as load following generators. It is assumed that all conventional generators connected in the system are load following generators which are able to supply power in their participation factor. In the assessment of HBSM, an uniform increase in loading factor λ is taken for simplicity. However, non-uniform load increase scenario can also be accounted. For the given load factor 'λ', load and generation at i^{th} node can be calculated as

$$P_{Li}(\lambda) = P^p_{Li} \times (1+\lambda) \tag{10}$$

$$Q_{Li}(\lambda) = Q^p_{Li} \times (1+\lambda) \tag{11}$$

$$P_{Gj}(\lambda) = P^p_{Li} + \frac{P^p_{Gi}}{\sum_j^m P^p_{Gi}} \times \sum_i^n P^p_{Li}(\lambda) \tag{12}$$

Where, P_{Li} and Q_{Li} are the active and reactive power loads at node i; P_{Gj} is the generator connected at node j. Base case operating point is denoted by super subscripts 'p'. Incremental load is distributed among generators using the generation participation factor which is given in (12). 'm' and 'n' denote the number of generators and loads connected in the system.

4. Problem formulation

4.1. Objective function

For the Hopf bifurcation study, it is necessary to perform a series of load flows and eigenvalue analysis of the system (3) as the parameters slowly vary. The look-ahead method is formulated for the effective setting of the control parameters including Automatic Voltage Regulators (AVR) set point and Online Tap Changing (OLTC) transformer's taps. In this section, rescheduling of generator AVRs and OLTC taps under their specified limits is formulated as an optimization problem for the maximization of HBSM (λ_{HBSM}). The proposed rescheduling strategy can effectively respond to power system uncertainties due to forecasted load and RES. Optimal control rescheduling is achieved by solving the minimization of boundary power loss problem as in (13). Modelling of boundary power loss P_{BLoss} is derived in the subsequent subsections.

$$Min\ P_{BLoss} = P(y, U, \mathscr{L}) \tag{13}$$

Subject to

$$g(y, U) = 0 \tag{13a}$$

$$P^{min}_G(I) \le P_G(I) \le P^{max}_G(I);\ I \in generator - bus \tag{13b}$$

$$Q^{min}_G(I) \le Q_G(I) \le Q^{max}_G(I);\ I \in generator - bus \tag{13c}$$

$$V^{min}_{load}(I) \le V_{load}(I) \le V^{max}_{load}(I);\ I \in load - bus \tag{13d}$$

$$U^{min}(k) \le U(k) \le U^{max}(k);\ k \in controller \tag{13e}$$

$$Re\{\mu_c\} \le 0 \tag{13f}$$

Where, $P(y, U, \mathscr{L})$ is the total boundary active power loss, calculated at optimal settings of control variables U. The power balance equality constraints are enforced in (13a). The active and reactive powers generated by individual generators are bounded using (13b) and (13c), respectively. The $V_{load}(I)$ is the voltage magnitude at I^{th} load bus. $Q_G(I)$ is the reactive power supplied by I^{th} generator. $U(k)$ is the k^{th} control variable. Subscripts 'min' and 'max' show the minimum and maximum permissible values of the associated parameters. In this paper generator voltages and taps of OLTC are selected as the reactive power control variables. System dynamics are considered in (13f), where μ_c is the lower boundary value of right-most critical mode. The problem formulation, however, can be solved using any meta-heuristic algorithm. Here, it is solved by a simple GWO algorithm [36].

Boundary values of both active power loss and eigenvalues for the specified range of forecasted load/generation data are required in the solution of (13). Formulation of the boundary power loss calculation is proposed in the following subsection. Note that boundary value calculation starts with deterministic solutions [14].

4.2. Deterministic active power loss calculation

Deterministic Load Flow (DLF) solution of the power system is obtained by solving set of non-linear power flow equations (14) using Newton Raphson (NR) method.

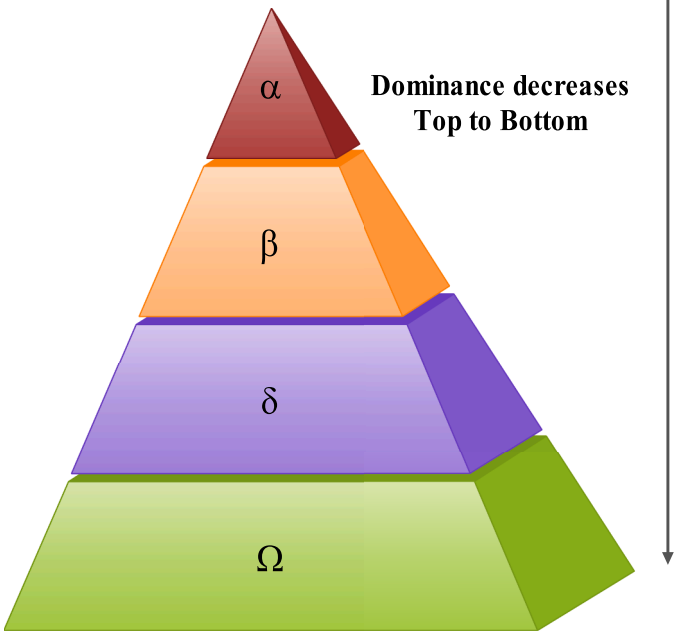

Fig. 2. Hierarchy of grey wolf in their pack

$$u = g(y, U) \tag{14}$$

where u is the vector of predefined input variable and y is the vector of unknown load flow state variable. U is set of control parameters. Equation (14) is linearised and solved iteratively as follows

$$\begin{cases} \Delta y = J^{-1}\Delta u \\ \Delta u = u_{sp} - u_c \end{cases} \tag{15}$$

Where J is the Jacobian matrix. Δy is the correction vector. u_{sp} is the specified input vector and u_c is the vector of function value u calculated at updated voltages. Vector y is updated through Δy in each iteration. Iteration is continued till the convergence value Δu became less than the specified tolerance ϵ. With the final value y, crisp active power loss can be evaluated as

$$P_{Loss} = Re\left(\sum_{i}^{n} V_i^* \sum_{j=1}^{n} V_j Y_{ij}\right) \qquad \forall \;\; i,j = 1,2,3...n \tag{16}$$

Where V_i and V_j are voltage at i^{th} and j^{th} bus respectively in the 'n' bus power system. Y_{ij} is the element of Y_{bus}.

4.3. Boundary Active Power Loss (BAPL) calculation

For the specified range of load ($[P_{Lmin}, P_{Lmax}]$) at each bus, extreme boundaries of active power loss are obtained. Evaluation of boundary active power loss (BAPL) is based on boundary load flow which always starts with deterministic load flow solutions and P_{loss}. Details of the deterministic solutions and boundary power flow are not given here however one can find it in [18]. Generations corresponding to load vector can be obtained using generator participation factors as given in (12).

The upper/lower value of BAPL (P_{Bloss}) for a given range of uncertainty is obtained as follows.

$$P_{Bloss} = P^{e}_{Loss} + L \times \left(P_{Lsp} - P_{Le}\right) \tag{17}$$

Where, L is the sensitivity matrix of active power loss with respect to load P_L at a bus. Sensitivity matrix L is calculated in (18). P_{Lsp} is the selected load vector from the pre-specified interval (upper and lower) which depends on the sign of the associated element of L. P_{Le} is the current estimate of loads. P^{e}_{Loss} is the current estimate of P_{Loss} evaluated at $P_L = P_{Le}$.

$$L = \frac{\partial P_{Loss}}{\partial P_L} = \left[\frac{\partial P_{Loss}}{\partial \delta}\right] \times \left[\frac{\partial \delta}{\partial P_L}\right] + \left[\frac{\partial P_{Loss}}{\partial V}\right] \times \left[\frac{\partial V}{\partial P_L}\right] \tag{18}$$

If the upper bound of P_{Loss} is of interest, then $P_{Loss_i} = P_{Lmax_i}$ when L_i is positive. Similar logic holds true if the lower bound of P_{Loss} is of interest. It is important to note that role of (17) is only for input vector selection using loss sensitivity and not for calculation of actual P_{Bloss}. With the selected input, actual P_{Bloss} is evaluated from (16). This completes one execution of BAPL.

BAPL is minimized via the optimal set of controls. With obtained BAPL solution and set of controls, critical boundary eigenvalues for the current loading are calculated. Similar calculations are made for every load steps till $\sigma_{crit} < 0$. The values of load step where σ_{crit} crosses the imaginary axis are noted as λ_{HB} for the selected setting. This boundary-value calculation helps to evaluate the HBSM.

4.4. Gray Wolf Optimization Algorithm

4.4.1. Overview

In this problem, controls are varying in discrete steps, so a meta-heuristic technique will be more feasible for the optimization process. The control variables are optimized using a grey wolf optimization (GWO) algorithm developed by Mirjalili and Lewis [36] in 2014. This algorithm is inspired by two interesting behaviours, group hunting and leadership hierarchy of grey wolves (Canis Lumps) pack. Pack of four types of wolves such as Alpha (α), Beta (β), Delta (δ), and Omega (Ω) is dictated by alphas. The strict leadership hierarchy is shown in Fig. 2. All social and hunting decisions are taken by the pack leaders (α). The three phases of group hunting mechanism are given as-

- Tracking, chasing and approaching the prey.
- Pursuing, encircling, and harassing the prey until it stops moving.
- Attack towards the prey.

4.4.2. Mathematical model and algorithm of GWO

In order to develop the GWO algorithm, the social and hunting behaviour of the grey wolves is mathematically modelled.

$$\vec{D} = |\vec{C} \cdot \vec{z}_p(t) - \vec{z}(t)| \tag{19}$$

$$\vec{z}(t+1) = \vec{z}_p(t) - \vec{A}_c \cdot \vec{D} \tag{20}$$

Where, t is the iteration number. $\vec{z}$ and $\vec{z}_p$ are the vector of position of grey wolves and the prey respectively. Coefficient vectors "$\vec{A}_c$" and "$\vec{C}$" can be calculated by the following equations.

$$\vec{A}_c = 2\vec{a} \cdot \vec{r}_1 - \vec{a} \tag{21}$$

$$\vec{C} = 2 \cdot \vec{r}_2 \tag{22}$$

Random vectors r_1 and r_2 are in $[0,1]$. In order to simulate the hunting (optimizing) behaviour of grey wolves (solution candidates), the three best solution candidates are selected as α, β, and δ. The rest of the solution candidates (Ω) are allowed to update their positions according to the position of the best solution candidates. Mathematically it can be expressed as-

$$\begin{cases} \vec{D}_\alpha = |\vec{C}_1 \cdot \vec{z}_\alpha - \vec{z}|, \\ \vec{D}_\beta = |\vec{C}_2 \cdot \vec{z}_\beta - \vec{z}| \\ \vec{D}_\delta = |\vec{C}_3 \cdot \vec{z}_\delta - \vec{z}| \end{cases} \tag{23}$$

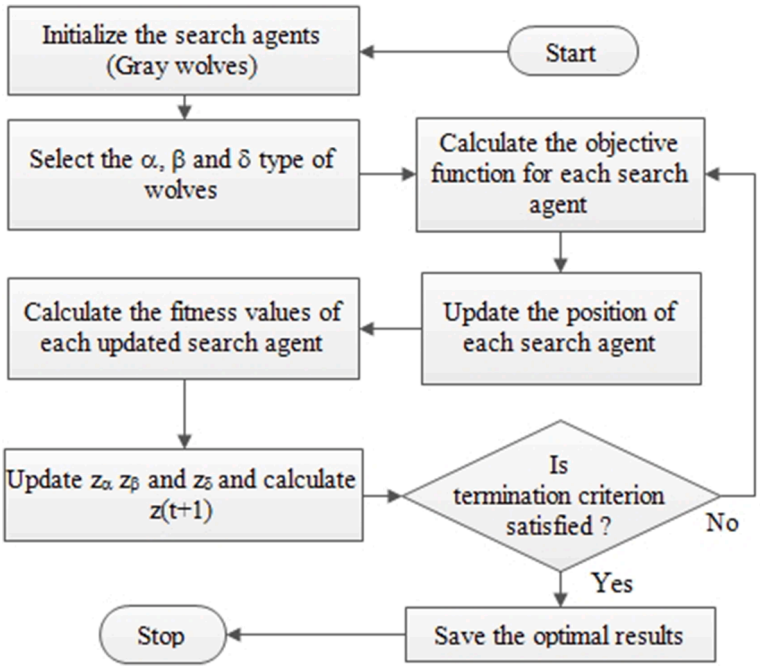

Fig. 3. GWO algorithm flow chart

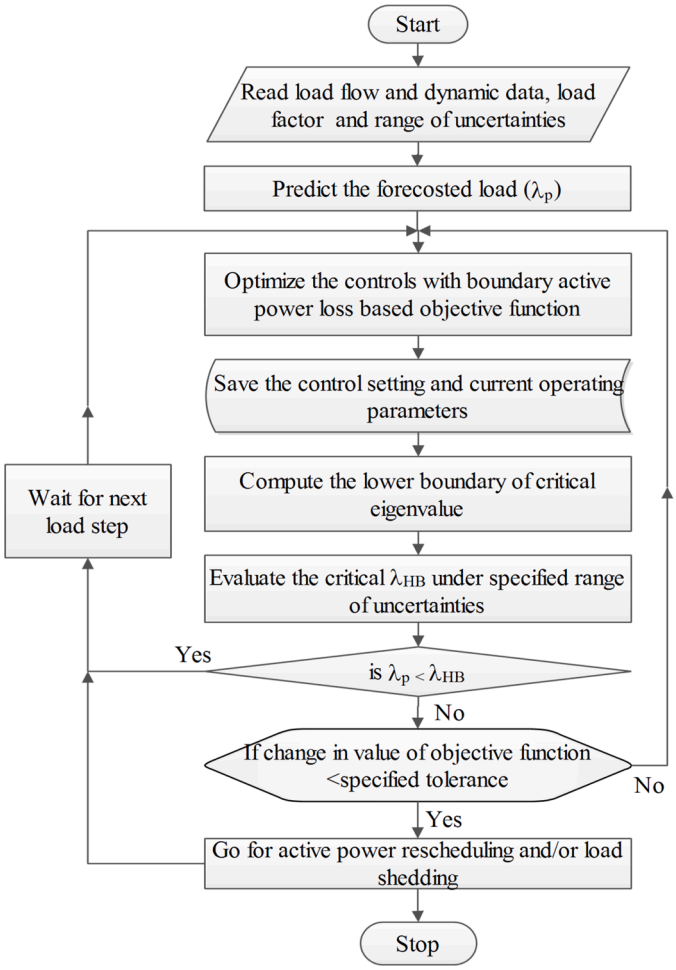

Fig. 4. Flow Chart

$$\begin{cases} \vec{z}_1 = |\vec{z}_\alpha - \vec{A}_{c1}\cdot\left(\vec{D}_\aleph\right)|, \\ \vec{z}_2 = |\vec{z}_\beta - \vec{A}_{c2}\cdot\left(\vec{D}_\beta\right)|, \\ \vec{z}_3 = |\vec{z}_\delta - \vec{A}_{c3}\cdot\left(\vec{D}_\delta\right)|, \end{cases} \tag{24}$$

$$z(t+1) = \frac{\vec{z}_1 + \vec{z}_2 + \vec{z}_3}{3} \tag{25}$$

GWO algorithm starts with generating random positions of grey wolves in the candidate solution space. Over the progress of iterations, the position of prey (optimum solution) is estimated by α, β, and δ wolves. Each wolf (solution candidate) updates its distance according to the estimated position of prey. Exploration and exploitation can be handled by decreasing the value of 'a' in (21) from 2 to 0. Convergence/divergence of candidate solution depends on the value of '$\vec{A_c}$'. That means the adaptive value of the 'a' and $\vec{A_c}$ allow GWO to have a smooth transition between exploration and exploitation. For $|\vec{A_c}| < 1$, it is converged towards the prey. Whereas, it is diverged from the prey if $|\vec{A_c}| > 1$. Finally, the algorithm is terminated by specified termination conditions. The flow chart of the GWO algorithm is given in Fig. 3.

4.5. Look-ahead approach for updating control settings

The flow chart of the proposed approach is given in the Fig. 4. The important steps in this algorithm are described as follows-

Step 1: Read the operating and dynamic data of the system with a specified range of uncertainties

Step 2: Using load/generation forecast predict the next load step

Step 3: Specify the range of forecasted load/generation uncertainties at each node.

Step 4: Solve boundary power loss optimization for setting an effective control parameters and references using boundary value approach explained in the subsection 4.3.

Step 5: Compute the critical eigenvalue and evaluate HB point (λ_{HB}) using boundary eigenvalue approach as described in subsection 3.3.

Step 6: If λ_{HB} is greater than predicted load, wait for the next

Table 1
OPTIMAL CONTROL SETTING OF WSCC, 9 BUS SYSTEM WITHOUT SPVG

	Optimal values of control parameters					
	Line No.	Taps	Gen. Bus	Gen. Volt. (p.u)	Critical loading & eigenvalue with proposed optimal control	Critical loading & eigenvalue without optimization [1]
Without uncertainties	1-4	0.95	1	1.10	$\lambda_{HB} = 1.2, \sigma_{crit} = -0.0097$	$\lambda_{HB} = 0.87, \sigma_{crit} = -0.0055$
	2-7	0.96	2	1.094		
	3-9	0.99	3	1.096		
With±5 % uncertainty	1-4	0.97	1	1.072	$\lambda_{HB} = 0.995, \sigma_{crit} = -0.1931 \sigma_{crit\_lower\_b} = -0.0087 \sigma_{crit\_lower\_b} = -0.0083$	$\lambda_{HB} = 0.78, \sigma_{crit} = -0.1955$
	2-7	0.98	2	1.072		
	3-9	0.99	3	1.074		

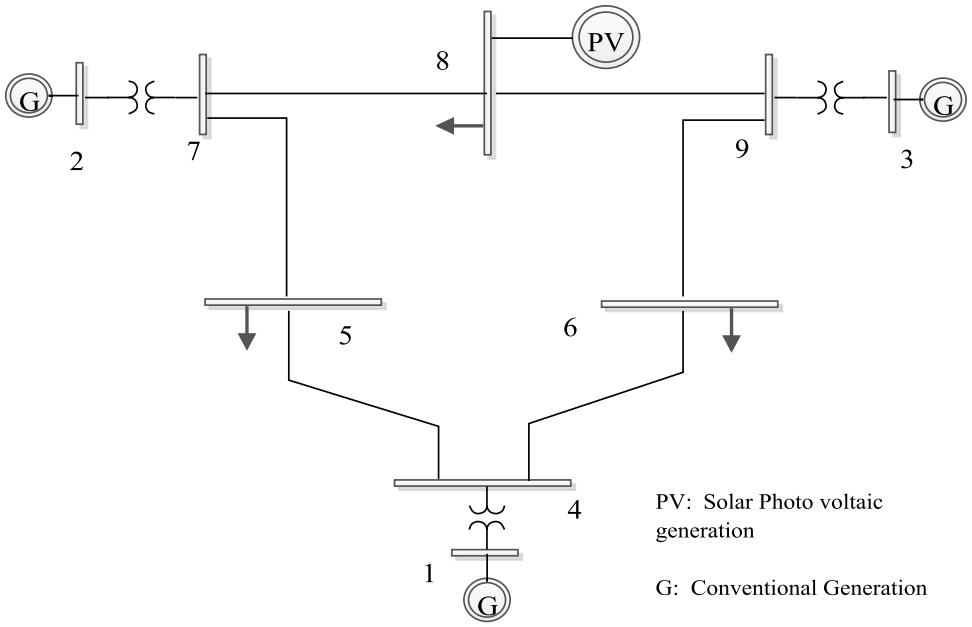

Fig. 5. Modified WSCC, 3-machine, 9-bus test system

predicted load and go to step 1.

Step 7: If the predicted load is more than λ_{HB}, check whether the difference in margin of two successive steps is greater than the specified tolerance. If yes, update the controls and repeat the process from step 3. Otherwise, go to next step.

Step 8: Ready for emergency control action like active power rescheduling and /or load shedding if required.

In the proposed approach, uncertainties are considered in loads and SPVGs only. It is assumed that conventional generators are capable to meet the required power demand as all generators in the system are load following generators and can be rescheduled for each operating time interval. The generation participation factors evaluated in (10) at crisp data are utilized to distribute the demanded loads among the conventional generators. Since it is difficult to derive the relationship between control settings and HBSM due to discussed non-linearities, it appears that the proposed method is a simple and alternate solution to prevent or postpone the HB instability even in presence of load/generation uncertainties. The main concept of this approach is to obtain the optimal schedule of controls for the next predicted load with possible uncertainties. This approach requires little more computing time than the deterministic approach because of the additional sensitivity calculations to accommodate the uncertainties in the evaluation of boundary values of active power loss and critical eigenvalue. However, this approach gives a realistic HBSM to the system analyst and helps it to prepare measures for the worst-case scenarios.

5. Results and Discussions

Proposed stability enhancement approach has been demonstrated with IEEE standard test systems: (i) Western System Coordinating Council (WSCC), 3-machine, 9-bus [32] and (ii) New England, 10-machine, 39-bus system [37] and (iii) 24-Machine 203-bus system [38]. In the simulation studies, two different cases, without and with solar photovoltaic (PV) integration, are considered at few buses to account for the generation uncertainties. The generators equipped with IEEE type-I exciter adopt the detailed DAE model (7th order). All loads adopt the classical static model. In terms of size, complexity, and SPVG penetration, each test system has different operating characteristics which is sufficient to examine the generalized effects of control rescheduling under various uncertainties. All simulation works are performed in MATLAB software.

5.1. WSCC system (3-machine, 9-bus)

This test system consists of 3 machines connected with OLTC transformers, 3 loads, and 6 transmission lines. The system has a total of 9-buses. In the base case, the total active and reactive power load in the system is 315 MW and 115 MVAr, respectively. Detailed dynamic data of generator, exciter, and network is given in Appendix-A. For simplicity, the uncertainty range in forecasted data at each node is considered to be ±5%. However, different uncertainty range at each node can be considered. Settings of static controllers, generator voltage reference (V), and taps of OLTC transformers (T) are optimized to improve the HBSM. All load demand and the scheduled real power generation of

Table 2
CONTROLLER PARAMETER SETTINGS OF WSCC, 9 BUS SYSTEM WITH SPVG

	Optimal values of control parameters					
	Line No.	Taps	Gen. Bus	Gen. Volt. (p. u)	Critical loading & eigenvalue with proposed optimal control	Critical loading & eigenvalue without optimization [1]
					with proposed optimal control	without optimization [1]
Without uncertainties	1-4	0.95	1	1.10	$\lambda_{HB} = 1.335$, $\sigma_{crit} = -0.0075$	$\lambda_{HB} = 0.95$, $\sigma_{crit} = -0.0221$
	2-7	0.95	2	1.098		
	3-9	0.99	3	1.10		
With±5 % uncertainty	1-4	0.97	1	1.07	$\lambda_{HB} = 1.05$, $\sigma_{crit} = -0.2034$	$\lambda_{HB} = 0.85$, $\sigma_{crit} = -0.2215\sigma_{crit} = -0.0221$
	2-7	0.96	2	1.054	$\sigma_{crit\_lower\_b} = -0.0028$	
	3-9	0.97	3	1.049		

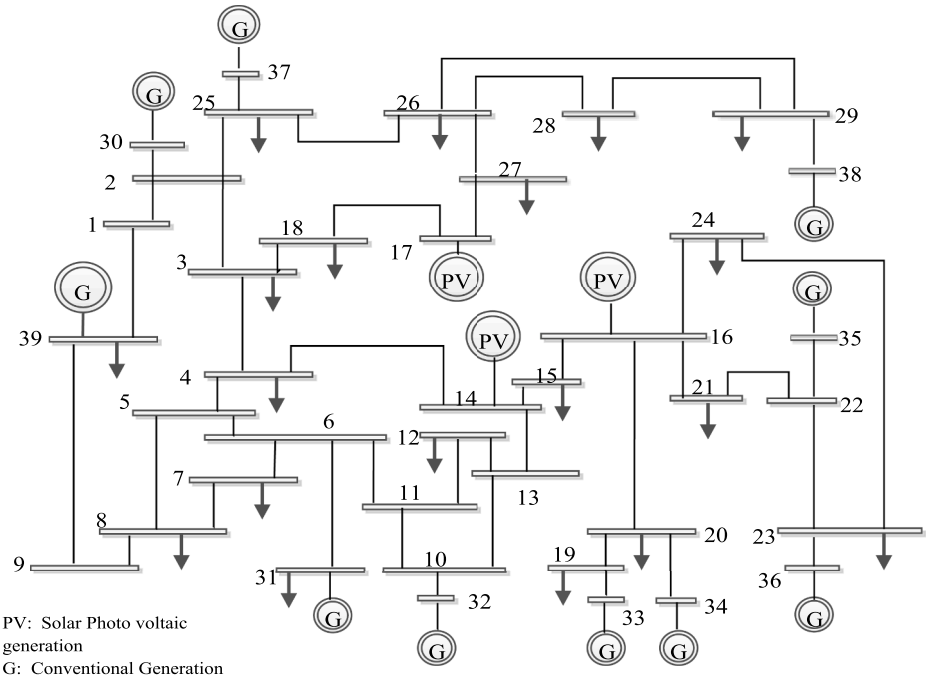

Fig. 6. Modified New England, 10-machine, 39-bus test system

look-ahead forecasting point are the same percentages. The bifurcation parameter λ is used to model the power load variation at all nodes i.e., given in (3)-(10). The Hopf bifurcation of the look-ahead point is directly calculated from the state-space model of the system given in (2), (11)-(12) using the selected control parameters and reference settings. Dynamics of the system are accounted in this DAE model, and hence in the critical eigenvalues. The results for two different cases are presented with IEEE 9-bus system.

5.1.1. WSCC system without SPVG

In this case, the BAPL and critical eigenvalues of the system without SPVG penetration are evaluated. Reactive power generation limits of the generators connected in the WSCC system are considered as 0.9 lead/lag power factor of the specified capacity of associated generators. Minimum and maximum generated voltages are bounded by excitation system from 0.9 to 1.1 pu respectively for each voltage-controlled bus. The tap setting of OLTC transformers can be adjusted between 0.95 to 1.05 pu. The permissible minimum and maximum voltages at load buses are assumed to be 0.9 and 1.10 pu, respectively.

The optimized reference values of generator voltage and OLTC tap settings are enumerated in Table 1. It can be seen that when uncertainties are not considered (deterministic approach), HB point (λ_{HB}) and critical eigenvalue of the system with optimal control setting is obtained as 1.2 and -0.0097, respectively. Whereas, with forecasted uncertainties of ± 5 %, critical value of λ_{HB} and boundary eigenvalue ($\sigma_{crit,lower\_b}$) are evaluated as 0.995 and -0.0087, respectively. λ_{HB} with uncertainties is lesser than the value without uncertainties. This HB limit is more realistic to use for the power system operation & design so that system can handle even worst-case scenarios in the uncertain power system. The results obtained in this table are also compared with the results in [1], which are calculated on nominal values of references voltages and taps. It can be seen that rescheduling of control settings within their limits significantly improves the loadability of the system. It can be observed that without uncertainty, HBSM is enhanced from 0.87 to 1.2, and also, with uncertainties, a significant HBSM enhancement has been achieved from 0.78 to 0.995.

5.1.2. WSCC system with SPVG

An SPVG of 20 MW is assumed at the 8th node in the WSCC system as shown in Fig. 5. Thus, the peak penetration level of the system is up to 7%. The range of uncertainty in SPVG and loads is assumed to be ± 5 %. With the integration of SPVG, the stability margin of the system has increased, and accordingly, the uncertainty level of the system has also increased. Obtained results for the system are given in Table 2. It shows that HBSM with uncertainty is reduced to 1.05 (i.e. 21.34 % of the case without uncertainty) from $\lambda_{HB} = 1.335$. The real part of critical

Table 3
OPTIMAL CONTROL OF NEW ENGLAND, 39 BUS SYSTEM WITHOUT SPVG

	Optimal values of control parameters					
	Line No.	Taps	Gen. Bus	Gen. Volt. (p. u)	Critical loading & eigenvalue with proposed optimal control	Critical loading & eigenvalue without optimization [1]
Without uncertainties	12-11	0.96	30	1.045	$\lambda_{HB} = 0.757$, $\sigma_{crit} = -0.0041$	$\lambda_{HB} = 0.553$, $\sigma_{crit} = -0.007$
	12-13	0.95	31	1.092		
	6-31	1.07	32	1.096		
	10-32	1.07	33	1.089		
	19-33	1.04	34	1.082		
	20-34	1.01	35	1.053		
	22-35	1.08	36	1.09		
	23-36	1.01	37	1.087		
	25-37	1.02	38	1.099		
	2-30	1.04	39	1.076		
	29-38	0.99	–	–		
	19-20	1.02	–	–		
With±5 % uncertainty	12-11	0.96	30	0.936	$\lambda_{HB} = 0.646$, $\sigma_{crit} = -0.3285\sigma_{crit\_lower\_b} = -0.0042$	$\lambda_{HB} = 0.48$, $\sigma_{crit} = -0.3212\sigma_{crit\_lower\_b} = -0.0007$
	12-13	1.06	31	1.071		
	6-31	1.05	32	1.071		
	10-32	1.02	33	1.091		
	19-33	1.02	34	1.095		
	20-34	1.08	35	1.038		
	22-35	1.00	36	1.1		
	23-36	1.00	37	1.093		
	25-37	1.09	38	1.099		
	2-30	0.97	39	1.077		
	29-38	1.00	–	–		
	19-20	0.96	–	–		

Table 4
OPTIMAL CONTROL OF NEW ENGLAND, 39 BUS SYSTEM WITH SPVG

	Optimal values of control parameters					
	Line No.	Taps	Gen. Bus	Gen. Volt. (p. u)	Critical loading & eigenvalue with proposed optimal control	Critical loading & eigenvalue without optimization [1]
Without uncertainties	12-11	0.98	30	0.971	$\lambda_{HB} = 0.873$, $\sigma_{crit} = -0.0088$	$\lambda_{HB} = 0.7$, $\sigma_{crit} = -0.0607$
	12-13	0.99	31	1.067		
	6-31	1.07	32	1.028		
	10-32	1.09	33	1.098		
	19-33	1.01	34	1.089		
	20-34	0.99	35	1.038		
	22-35	1.07	36	1.067		
	23-36	1.04	37	1.008		
	25-37	1.07	38	1.099		
	2-30	0.99	39	1.073		
	29-38	0.97	–	–		
	19-20	1.02	–	–		
With±5 % uncertainty	12-11	0.96	30	0.961	$\lambda_{HB} = 0.774$, $\sigma_{crit} = -0.1473\sigma_{crit\_lower\_b} = -0.0051$	$\lambda_{HB} = 0.61$, $\sigma_{crit} = -0.3474\sigma_{crit\_lower\_b} = -0.008$
	12-13	0.97	31	1.080		
	6-31	1.09	32	1.044		
	10-32	1.07	33	1.088		
	19-33	1.01	34	1.083		
	20-34	0.97	35	1.054		
	22-35	1.06	36	1.011		
	23-36	1.08	37	1.096		
	25-37	0.99	38	1.073		
	2-30	0.98	39	1.068		
	29-38	1.00	–	–		
	19-20	1.05	–	–		

Table 5
HB STABILITY ASSESSMENT OF 24-MACHINE 203 BUS SYSTEM

Cases	Critical loading & eigenvalue with normal control settings	Critical loading & eigenvalue with optimal control settings	Elapsed Time (s)
Without Uncertainties	$\lambda_{HB} = 4.57$, $\sigma_{crit} = -0.0009$	$\lambda_{HB} = 5.53$, $\sigma_{crit} = -0.0017$	41.286
With Uncertainties	$\lambda_{HB} = 3.95$, $\sigma_{crit} = -0.1988$	$\lambda_{HB} = 4.73$, $\sigma_{crit} = -0.1268$	58.879
	$\sigma_{crit\_lower\_b} = -0.006$	$\sigma_{crit\_lower\_b} = -0.0013$	

Table 6
ELAPSED TIME OF ALL TEST SYSTEMS

S. No	System description	Elapsed Time (In seconds)		
		Identification of critical mode	Assessment of HBSM with Optimal setting of controllers	Total time
1	3-machine 9-bus	0.131	1.386	1.517
2	10-machine 39-bus	0.162	2.239	2.401
3	24-machine 203-bus	0.462	58.417	58.879

eigenvalues with crisp and forecasted data at critical loadings are also given in the table as - 0.2024 and -0.0028 respectively.*Impact of the proposed control setting is verified by comparing HBSM values obtained in Table 2 with the corresponding results discussed in [1] where fixed control parameters were taken. In presence of SPVG, HBSM is considerably improved from 0.85 to 1.05 under specifies ± 5 % load/generation uncertainties.*

5.2. New England system(10-machine, 39-bus)

The interconnected New England, 39-bus test system contains 10 generators, 46 lines, and 20 loads. A two-axis model of the generators connected in the system is adopted in the DAE modelling. Detailed test system data is taken from [37]. A single line diagram of the test system is depicted in Fig. 6. Total 195 variables including 70 state variables for the system are investigated under a specified range of uncertainties. The uncertainty range at each bus is assumed to be ± 5 % to demonstrate the effectiveness of the proposed approach. Limits of various power system parameters are accounted during the optimal setting of generator voltage reference and OLTC taps settings. Considered reactive power limits of the generators connected in 39 bus systems are calculated from 0.9 lead/lag power factor of the specified capacity of associated generators. Generator reference voltages are controlled between 0.9 to 1.1 pu. Whereas, tap control of OLTC transformers is adjusted between 0.95 to 1.15 pu. In the simulation, load bus voltages are bounded to be between 0.9 to 1.10 pu.

5.2.1. New England system without SPVG

For this system, the optimal settings of the generator reference voltage and OLTC taps with and without consideration of uncertainties are given in Table 3. The maximum value of HBSM is found to be 0.757 when uncertainties are not considered. As we already discussed that under the uncertainties, the operating point of the system may change. In this scenario, the optimal setting of the controllers is required to be rescheduled to achieve the maximum HBSM. Optimal settings of voltages and taps under ± 5 % uncertainties are also given in the table. With this control setting, HBSM is achieved to be 0.646. Due to uncertainties, this value is less than the value obtained without uncertainties, but it is more realistic to take control actions keeping uncertainties in mind. Critical boundary and crisp eigenvalues for specified ± 5 % uncertainties in forecasted data are given in Table 3. System dynamics are accounted in the calculation of critical eigenvalues. The results with the proposed approach are compared with results in [1] where fixed control parameters and voltage references were considered. It is found that the stability margin λ_{HB} of the system is enhanced by 34.58 % (i.e. λ_{HB}=0.48 to 0.646) by the optimal setting of the static controllers.

5.2.2. New England system with SPVG

In this section, three SPVG units having 200 MW capacity (each) at unity power factor are integrated at three different buses 14th, 16th, and 17th, in the modified 39-bus system depicted in Fig. 6. These SPVG units are considered as negative loads as explained in[35]. Similar to the previous cases, the level of uncertainties in load and SPVG forecast are specified at ± 5%. Results of two different optimization cases are given in Table 4. Critical loading scenarios at optimal settings of the control parameters are presented.

For the case ($\lambda = 0$) optimal control setting is effective to minimize the system active power loss under the specified range of uncertainty at each bus. Moreover, this control setting significantly improved the HBSM of the system. The results obtained with the proposed approach are given in Table 4. Critical loading of the system with and without uncertainties are evaluated as 0.774 and 0.873, respectively. As uncertainties in data are always present, the operator must use the HB limit as 0.774 instead of 0.873 for the secure and stable operation of the power systems. Boundary value of critical eigenvalue ($\sigma_{crit,lower\_b}$) at critical loading λ_{HBSM} is also given in the Table 4 as -0.0051. In this case, obtained critical loading of the system with SPVG is enhanced to λ_{HB} = 0.774 from corresponding value 0.61 given in [1] under various data uncertainties.

From the above results and discussions, we can observe that the stability of the system is increased with the integration of SPVG because loads are supplied locally. Due to locally available SPVG, the power supplied over the transmission lines and effective active power losses in the system is reduced. The operating scenario of the system with SPVGs is changed and the HBSM of the system is considerably increased. This approach can be also used to maximize the solar PV penetration in the power system under HB stability limit constraints.

5.3. 24-machine, 203-bus test system

The objective of this case study is to show the calculation efficiency and requirement of consideration of estimated/forecasted data uncertainties in HBSM assessment. The proposed approach has been demonstrated with a large-scale 203-bus power system composed of 159 transmission lines, 35 line-transformer, 37 load-transformer, 24-generators, and 111-loads. This system has 14 areas. All generators adopt a comprehensive 7-order DAE model. In this case study, It is assumed that a total of 35-OLTC transformers and 24 voltage-controlled buses are available for rescheduling. Detailed dynamic data of generator, exciter, and transmission lines parameters are given in [38]. The DAE model of the system is the one presented in the above section respecting the characteristics of this system at different operating points. The bifurcation parameter λ is used to model the load variation at all buses. For the demonstration, a uniform increase in load factor λ is considered in the HBSM assessment. For the predicted loading (λ) at the given look-ahead step, load and generation at each bus can be evaluated using (10)-(12).

In this case, BAPL and critical eigenvalues are calculated without SPVG consideration. The worst-case scenario is evaluated using boundary eigenvalues with the specified uncertainty range of ± 5% at all. The setting of static controllers, generator voltage control, and taps of OLTC transformers are optimized to enhance the BHSM. Minimum and maximum generated voltages are bounded by excitation system from 0.9 to 1.1 pu respectively for each voltage-controlled bus. The tap setting of OLTC transformers can be adjusted between 0.95 to 1.05 pu. Other equality and inequality constraints are accounted during evaluation of the optimal setting of the controllers.

The results of a comprehensive study with four different cases are presented in Table 5. It can be seen that without consideration of uncertainties (Deterministic approach), HB loading (λ_{HB}) and critical eigenvalue (σ_{crit}) with nominal control setting are obtained as 4.57 and -0.0009 respectively. With the optimal setting of the controllers, λ_{HB} is enhanced to 5.53. Whereas, with forecasted uncertainties of ± 5 % and normal control settings, critical value of λ_{HB} and boundary eigenvalue ($\sigma_{crit,lower\_b}$) are evaluated as 3.95 and -0.1988, respectively. It is important to note that the value of λ_{HB} with uncertainties is lesser than the value without uncertainties. This HB limit is more realistic to use for the power system operation & design so that the system can handle even worst-case scenarios in the uncertain power system. The results obtained in this table are also compared with the results calculated on nominal values of references voltages and taps. It can be seen that rescheduling of control settings within their limits significantly improves the loadability of the system. It can be observed that without uncertainty, HBSM is enhanced from 4.57 to 5.53, and also, with uncertainties, a significant HBSM enhancement has been achieved from 3.95 to 4.73 by the

rescheduling of the controller's settings. Optimal settings of generator bus voltages and taps are given in Appendix-B

5.4. Discussion

Simulation work for all test systems was performed on a desktop computer with a 64-bit operating system, Intel®Core™M i5 CPU@1.70 GHz, 8 GB RAM, and 64-bit operating system. Calculation time for all the test systems is presented in Table 6. For identification of critical mode, the rightmost eigenvalues of the system matrix are calculated by increasing system loading λ in steps. As we discussed, in any power system analysis system parameter uncertainness must be accounted. Therefore, a boundary eigenvalue method is used for critical mode identification instead of a deterministic eigenvalue approach. This analytical method to account for the specified range of uncertainties is fast enough for online applications.

In addition, compared to a deterministic method, the proposed method has an obvious advantage in computing time and a realistic stability margin assessment. Taking the 10-machine, 39-bus system example, the total elapsed time for an online switching method presented in [2] is 1.73 without accounting for the parameter uncertainties. Whereas the proposed method without uncertainty takes only 1.29 seconds which is considerably less than the time taken in [2]. It is discussed in the above sections, parameters uncertainties must be considered in any power system analysis. The proposed method in presence of parameters uncertainties takes 2.401 seconds in the assessment and enhancement of HBSM which is reasonably acceptable for the online implementation.

The effectiveness of the boundary value-based look-ahead approach to enhance the HBSM depends on the accuracy of the estimated/forecasted load-generation data and rescheduling of static controllers. The proposed approach can be used for both deterministic and non-deterministic (uncertain) power system data. Comparatively a non-deterministic stability assessment takes little more calculation time but gives realistic HBSM information for operation and control.

6. Conclusions

In this paper, a boundary value-based look-ahead method is proposed for the enhancement of HBSM under the specified range of uncertainties in the forecasted/estimated load-generation data. An optimization algorithm has been used for rescheduling of the static controllers such as generator voltage references and taps of OLTC transformers. An active power loss-based optimization function has been developed for the uncertain power system where boundary load flow and boundary eigenvalue analysis methods are used accounting for the non-statistical uncertainties. This approach is inspired by boundary eigenvalue analysis to identify the worst-case scenario in the uncertain power system. It is an economical and effective approach to enhance the HB limits/HBSM. Indirectly minimization of BAPL makes the controllers focus on controlling the critical oscillatory modes of the system. The proposed method is capable of determining the HB limits of the stressed power system with simple calculations, which allows using this method for the real-time operation of the system. Case studies on 9-Bus, 39-Bus, and 203-Bus systems have been done to justify the potential benefits of the proposed approach. HBSM assessment and enhancement of uncertain power system are illustrated via numerical tests on 9-bus, 39-bus, and 203 bus power systems integrated with different sizes of distributed SPVGs.

Hopf bifurcation stability analysis in presence of uncertainty can be used for the optimal design of power system controllers and further can be used for the minimum power plant re-despatch to supply uninterrupted power. Hence it can be useful for the power system security assessment. Future research will evaluate the proposed method for power systems with network topologies such as online switching and contingency screening.

CRediT authorship contribution statement

Ram Krishan: Conceptualization, Methodology, Software, Data curation, Writing – original draft, Visualization, Investigation, Writing – review & editing. **Ashu Verma:** Supervision, Validation.

Declaration of Competing Interest

The authors declare that they have no known competing financial interests or personal relationships that could have appeared to influence the work reported in this paper.

Acknowledgments

The first author would like to thank Dr. Deepak Reddy Pullaguram, Dr. Sanjaya Kumar Panda, and Dr. Venkateswara Rao Kagita, NIT Warangal for their valuable discussions and support. This work was supported by the National Supercomputing Mission (NSM), Department of Science and Technologies (DST), India (Reference: DST/NSM/R&D_HPC_Applications/2021/03.31.).

Appendix A. WSCC 3-machine 9-bus test system data [32]

Network parameters, load flow data and dynamic data of the machines of the 3-machine, 9-bus system are given in Table A.1, A.2, A.3, A.4

Table A.1
Load and generation data of the WSCC 9-bus system

Bus No.	Bus Type	Voltage (pu)	Load (MW)	Load (MVAr)	Generation (MW)	Q_{max} (MVAr)	Q_{min} (MVAr)
1	Slack	1.04	0	0	0	100	-100
2	PV	1.025	0	0	163	100	-100
3	PV	1.025	0	0	85	100	-100
4	PQ	1	0	0	0	0	0
5	PQ	1	125	50	0	0	0
6	PQ	1	90	30	0	0	0
7	PQ	1	0	0	0	0	0
8	PQ	1	1	35	0	0	0
9	PQ	1	0	0	0	0	0

Table A.2
Transmission line data of WSCC 9-bus system

Line No.	Bus		Line resistance (pu)	Line reactance (pu)	B/2 (pu)	Transformers tap
	From	To				
1	1	4	0	0.0576	0	1
2	2	7	0	0.0625	0	1
3	3	9	0	0.0586	0	1
4	4	5	0.01	0.085	0.088	1
5	4	6	0.017	0.092	0.079	1
6	5	7	0.032	0.161	0.153	1
7	6	9	0.039	0.17	0.179	1
8	7	8	0.0085	0.072	0.0745	1
9	8	9	0.0119	0.1008	0.1045	1

Table A.3
Generator parameter of WSCC, 3-machine 9-bus system

Machine	Bus No	H (sec)	$X_d(pu)$	$X'_d(pu)$	$X_q(pu)$	$X'_q(pu)$	$T'_{d0}(sec)$	$T'_{q0}(sec)$
G1	1	23.64	0.146	0.0608	0.0969	0.0969	8.96	0.31
G2	2	6.4	0.8958	0.1198	0.8645	0.1969	6	0.535
G3	3	3.01	1.3125	0.1813	1.2578	0.25	5.89	0.6

Table A.4
Exciter data of WSCC, 3-machine 9-bus system

Generator	K_A	$T_A(sec)$	K_E	$T_E(sec)$	K_f	$T_f(sec)$
G1	20	0.2	1	0.314	0.063	0.35
G2	20	0.2	1	0.314	0.063	0.35
G3	20	0.2	1	0.314	0.063	0.35

Appendix B. 24-machine 203-bus system controllers

Optimal settings of generator bus voltages and taps in the 24-machine, 203 bus system is given in table-B.1.

Table B.1
OPTIMAL CONTROL OF 24- MACHINE 203 BUS SYSTEM

Optimal Taps setting			Optimal Voltage setting		
Line No.	Deterministic analysis	Uncertainty analysis	Gen. Bus	Deterministic analysis	Uncertainty Analysis
1-149	0.95	0.97	1	1.05	1.07
5-149	0.95	0.97	2	1.04	1.041
13-135	0.95	1.02	3	1.04	1.04
20-156	0.988	1.01	4	1.04	1.05
25-157	0.988	1.01	5	1.05	1.051
36-201	1.05	1.034	6	1.043	1.047
39-194	1.05	1.04	7	1.02	1.024
53-162	1.05	1.047	8	1.00	1.03
54-195	1.05	1.05	9	1.02	1.022
55-199	1.05	1.048	10	1.00	1.013
55-199	1.05	1.048	11	1.01	1.01
64-196	1.05	1.039	12	1.00	0.991
64-196	1.05	1.039	13	1.01	1.01
77-197	1.05	1.042	14	1.02	1.030
77-197	1.05	1.042	15	1.02	1.033
86-198	1.05	1.045	16	1.02	1.033
92-200	1.05	1.04	17	1.04	1.053
111-164	1.05	1.043	18	1.03	1.04
116-27	0.95	0.98	19	1.03	1.04
123-125	1.00	1.01	20	1.04	1.046
128-36	0.95	0.97	21	1.02	1.029
145-115	0.95	0.95	22	1.02	1.026
146-116	0.95	0.95	23	1.02	1.021
150-119	1.05	1.048	24	1.00	1.023
155-143	1.05	1.04	* The maximum and minimum limits of the load bus voltages are ± 10% i.e. 1.10 p.u. and 0.9 p.u.		
164-163	1.00	0.99			
177-120	1.00	0.95			
180-124	1.00	0.97	** The minimum and maximum limits of the transformer's tap is 0.95 p.u. and 1.05 p.u, respectively		
183-127	1.00	1.01			
191-137	1.00	1.00			

References

[1] R. Krishan, A. Verma, S. Mishra, P.R. Bijwe, Analysis of hopf bifurcation with forecast uncertainties in load/generation, IET Generation, Transmission Distribution 11 (6) (2017) 1531–1538, https://doi.org/10.1049/iet-gtd.2016.1316.

[2] C. Li, H. Chiang, Z. Du, Online line switching method for enhancing the small-signal stability margin of power systems, IEEE Transactions on Smart Grid 9 (5) (2018) 4426–4435, https://doi.org/10.1109/TSG.2017.2656885.

[3] C. Li, C. Duan, Y. Cao, An efficient method for computing exact delay-margins of large-scale power systems, IEEE Transactions on Power Systems 35 (6) (2020) 4924–4927, https://doi.org/10.1109/TPWRS.2020.3009848.

[4] Z. Yun, X. Cui, Online preventive control method for static voltage stability of large power grids, IEEE Transactions on Power Systems 35 (6) (2020) 4689–4698, https://doi.org/10.1109/TPWRS.2020.3001018.

[5] S. Mishra, M. Tripathy, J. Nanda, Multi-machine power system stabilizer design by rule based bacteria foraging, Electric Power Systems Research 77 (12) (2007) 1595–1607, https://doi.org/10.1016/j.epsr.2006.11.006.

[6] R. Krishan, A. Verma, An efficient approach to tune modern power system stabilizers using harmony search. 2015 Annual IEEE India Conference (INDICON), 2015, pp. 1–6, https://doi.org/10.1109/INDICON.2015.7443794.

[7] T. Surinkaew, I. Ngamroo, Coordinated robust control of dfig wind turbine and pss for stabilization of power oscillations considering system uncertainties, IEEE Transactions on Sustainable Energy 5 (3) (2014) 823–833, https://doi.org/10.1109/TSTE.2014.2308358.

[8] Y. Chen, S.M. Mazhari, C.Y. Chung, S.O. Faried, B.C. Pal, Rotor angle stability prediction of power systems with high wind power penetration using a stability index vector, IEEE Transactions on Power Systems 35 (6) (2020) 4632–4643, https://doi.org/10.1109/TPWRS.2020.2989725.

[9] J.N. da Costa, J.A. Passos Filho, R. Mota Henriques, Loading margin sensitivity analysis in systems with significant wind power generation penetration, Electric Power Systems Research 175 (2019) 105900, https://doi.org/10.1016/j.epsr.2019.105900.

[10] P. Mandoulidis, C. Vournas, A PMU-based real-time estimation of voltage stability and margin, Electric Power Systems Research 178 (2020) 106008, https://doi.org/10.1016/j.epsr.2019.106008.

[11] M. Chávez-Lugo, C. Fuerte-Esquivel, V.J. Gutierrez-Martínez, A direct method for the computation of the oscillatory voltage stability boundary, Electric Power Systems Research 167 (2019) 163–170, https://doi.org/10.1016/j.epsr.2018.10.037.

[12] R.S. Tare, P.R. Bijwe, Look-ahead approach to power system loadability enhancement, IEE Proceedings - Generation, Transmission and Distribution 144 (4) (1997) 357–362, https://doi.org/10.1049/ip-gtd:19971099.

[13] N. Mithulananthan, C.A. Canizares, J. Reeve, G.J. Rogers, Comparison of pss, svc, and statcom controllers for damping power system oscillations, IEEE Transactions on Power Systems 18 (2) (2003) 786–792, https://doi.org/10.1109/TPWRS.2003.811181.

[14] R. Shah, N. Mithulananthan, K.Y. Lee, R.C. Bansal, Wide-area measurement signal-based stabiliser for large-scale photovoltaic plants with high variability and uncertainty, IET Renewable Power Generation 7 (6) (2013) 614–622, https://doi.org/10.1049/iet-rpg.2013.0046.

[15] H.D. Nguyen, K. Turitsyn, Robust stability assessment in the presence of load dynamics uncertainty, IEEE Transactions on Power Systems 31 (2) (2016) 1579–1594, https://doi.org/10.1109/TPWRS.2015.2423293.

[16] M.E. Bento, R.A. Ramos, An approach for monitoring and updating the load margin of power systems in dynamic security assessment, Electric Power Systems Research 198 (2021) 107365, https://doi.org/10.1016/j.epsr.2021.107365.

[17] J. Rommes, N. Martins, Computing large-scale system eigenvalues most sensitive to parameter changes, with applications to power system small-signal stability, IEEE Transactions on Power Systems 23 (2) (2008) 434–442, https://doi.org/10.1109/TPWRS.2008.920050.

[18] A. Dimitrovski, K. Tomsovic, Boundary load flow solutions. IEEE Power Engineering Society General Meeting, 2004. 1, 2004, p. 1165, https://doi.org/10.1109/PES.2004.1373033.

[19] P. Bijwe, M. Hanmandlu, V. Pande, Fuzzy power flow solutions with reactive limits and multiple uncertainties, Electric Power Systems Research 76 (1) (2005) 145–152, https://doi.org/10.1016/j.epsr.2005.05.002.

[20] K.W. Wang, C.Y. Chung, C.T. Tse, K.M. Tsang, Improved probabilistic method for power system dynamic stability studies, IEE Proceedings - Generation, Transmission and Distribution 147 (1) (2000) 37–43, https://doi.org/10.1049/ip-gtd:20000025.

[21] C.Y. Chung, K.W. Wang, C.T. Tse, R. Niu, Power-system stabilizer (pss) design by probabilistic sensitivity indexes (psis), IEEE Transactions on Power Systems 17 (3) (2002) 688–693, https://doi.org/10.1109/TPWRS.2002.800914.

[22] Z. Xu, Z.Y. Dong, P. Zhang, Probabilistic small signal analysis using monte carlo simulation. IEEE Power Engineering Society General Meeting, 2005 2, 2005, pp. 1658–1664, https://doi.org/10.1109/PES.2005.1489425.

[23] R. Preece, N.C. Woolley, J.V. Milanović, The probabilistic collocation method for power-system damping and voltage collapse studies in the presence of uncertainties, IEEE Transactions on Power Systems 28 (3) (2013) 2253–2262, https://doi.org/10.1109/TPWRS.2012.2227837.

[24] A. Schellenberg, W. Rosehart, J. Aguado, Cumulant-based probabilistic optimal power flow (p-opf) with gaussian and gamma distributions, IEEE Transactions on Power Systems 20 (2) (2005) 773–781, https://doi.org/10.1109/TPWRS.2005.846184.

[25] A. Verma, P.R. Bijwe, B.K. Panigrahi, Heuristic method for transmission network expansion planning with security constraints and uncertainty in load specifications. 2009 Transmission Distribution Conference Exposition: Asia and Pacific, 2009, pp. 1–4, https://doi.org/10.1109/TD-ASIA.2009.5357012.

[26] A. Mohapatra, P. Bijwe, B. Panigrahi, Unified boundary and probabilistic power flow, Electric Power Systems Research 116 (2014) 136–146, https://doi.org/10.1016/j.epsr.2014.05.015.

[27] J. Qiu, S.M. Shahidehpour, A new approach for minimizing power losses and improving voltage profile, IEEE Power Engineering Review PER-7 (5) (1987) 36–37, https://doi.org/10.1109/MPER.1987.5527240.

[28] C.J. Bridenbaugh, D.A. DiMascio, R. D'Aquila, Voltage control improvement through capacitor and transformer tap optimization, IEEE Transactions on Power Systems 7 (1) (1992) 222–227, https://doi.org/10.1109/59.141707.

[29] J.L.M. Ramos, A.G. Exposito, V.H. Quintana, Transmission power loss reduction by interior-point methods: implementation issues and practical experience, IEE Proceedings - Generation, Transmission and Distribution 152 (1) (2005) 90–98, https://doi.org/10.1049/ip-gtd:20041150.

[30] M.R. Salem, L.A. Talat, H.M. Soliman, Voltage control by tap-changing transformers for a radial distribution network, IEE Proceedings - Generation, Transmission and Distribution 144 (6) (1997) 517–520, https://doi.org/10.1049/ip-gtd:19971430.

[31] M. Shakarami, I. Faraji Davoudkhani, Wide-area power system stabilizer design based on grey wolf optimization algorithm considering the time delay, Electric Power Systems Research 133 (2016) 149–159, https://doi.org/10.1016/j.epsr.2015.12.019.

[32] M.A.P. Peter W. Sauer, Power system dynamics and stability, Pearson education, 2002.

[33] P. Kundur, Power system stability and control, McGraw-hill, 1994.

[34] C. Luo, V. Ajjarapu, Sensitivity-based efficient identification of oscillatory stability margin and damping margin using continuation of invariant subspaces, IEEE Transactions on Power Systems 26 (3) (2011) 1484–1492, https://doi.org/10.1109/TPWRS.2010.2098424.

[35] B. Tamimi, C. Cañizares, K. Bhattacharya, System stability impact of large-scale and distributed solar photovoltaic generation: The case of ontario, canada, IEEE Transactions on Sustainable Energy 4 (3) (2013) 680–688, https://doi.org/10.1109/TSTE.2012.2235151.

[36] S. Mirjalili, S.M. Mirjalili, A. Lewis, Grey wolf optimizer, Advances in Engineering Software 69 (2014) 46–61, https://doi.org/10.1016/j.advengsoft.2013.12.007.

[37] M.A. Pai, Energy function analysis for power system stability, Kluwer Academic Publication, 1989.

[38] D. Mondal, A. Chakrabarti, A. Sengupta, Power System Small Signal Stability Analysis and Control, Academic Press, 2014.